



# Linear Collider Collaboration Tech Notes

---

## Effects of Position and Angle Offsets on NLC Luminosity

June 10, 1999

K.A. Thompson and T.O. Raubenheimer  
Stanford Linear Accelerator Center  
Stanford, California

### Abstract:

We present simulation results for the luminosity reduction due to position and angle offsets in the beams colliding at the NLC interaction point. We look at the nominal NLC-B-500 and NLC-B-1000 designs and also at designs having the vertical beta function doubled at the IP.

# Effects of position and angle offsets on NLC luminosity

K.A. Thompson and T.O.Raubenheimer

The purpose of this note is to study the effect on luminosity of position and angle offsets in the beams colliding at the NLC interaction point.

Baseline NLC interaction point design parameters are as given on the NLC website [1] and a previous note [2]; for convenience we redisplay them in Table 1. In this note we shall focus on the NLC-B-500 and NLC-B-1000 designs and variations away from them. The GUINEAPIG beam-beam program [3] is used to simulate the beam-beam interaction.

An interesting result of a previous study [2] is that the luminosity (not only the total luminosity, but also the fraction of the luminosity near the nominal energy) is quite insensitive to variations in the vertical beta function. If the vertical beta function is increased by a factor of two from the nominal value, for zero-offset collisions one obtains a luminosity degradation of only 10% for NLC-B-500 and 15% for NLC-B-1000. The payoff for this luminosity loss is a loosening of tolerances in the final focus. In addition to quantifying the effects of offsets on the nominal NLC, another purpose of this note is to compare the effects of offsets in the relaxed beta function scenario.

If the charge is lowered from its nominal value, the disruption will be reduced further. Obviously the overall luminosity will go down when the charge is lowered. But we also wish to check how the luminosity degradation with offset is affected in the relaxed beta function case. Thus we also examine the case where the charge is reduced from the nominal value of  $N = 0.95 \times 10^{10}$  to  $0.8 \times 10^{10}$  (and the vertical beta function is doubled).

We show the results of scans in the full vertical offset (in units of the vertical beam size, except for Figures 4 and 12 in which the offset  $dy$  is given in nanometers) and scans in the crossing angle  $\theta_y$  [NOTE: this is the full angle between the beams, not the half-angle]. In all of Figures 1 through 8, the solid curve is for the nominal parameters (NLC-B-500 in Figures 1 through 8, and NLC-B-1000 in Figures 9 through 16), the dashed curve is for the vertical beta function doubled from its nominal value (i.e.  $\beta_y$  increased to 0.30 mm for NLC-B-1000, and  $\beta_y$  increased to 0.24 mm for NLC-B-500), and the dotted curve is for doubled vertical beta function and reduced charge (from the nominal value of  $N = 0.95 \times 10^{10}$  to  $0.8 \times 10^{10}$ ).

Figures 1 and 9 show the luminosity  $\mathcal{L}_D$  per bunch as the  $y$ -offset is varied. Figures 4 and 12 show the same thing, except that the  $y$ -offset is plotted in nanometers instead of in units of  $\sigma_y$ . Figures 2 and 10 show the luminosity enhancement factor  $H_D \equiv \mathcal{L}_D/\mathcal{L}_0$  where

**TABLE 1.** NLC IP parameters for baseline designs

	NLC-A-500	NLC-B-500	NLC-C-500	NLC-A-1000	NLC-B-1000	NLC-C-1000
$E_{beam}$ [GeV]	267.5	257.5	250.	523.	504.	489.
$N$ [ $10^{10}$ ]	0.75	0.95	1.1	0.75	0.95	1.1
$\gamma\epsilon_x/\gamma\epsilon_y$ [ $10^{-6}$ m-rad]	4.0/0.06	4.5/0.1	5.0/0.14	4.0/0.06	4.5/0.1	5.0/0.14
$\beta_x/\beta_y$ [mm]	10/0.1	12/0.12	13/0.2	10/0.125	12/0.15	13/0.2
$\sigma_z$ [ $\mu\text{m}$ ]	90.	120.	145.	90.	120.	145.
$\sigma_x/\sigma_y$ [nm]	276.43/3.39	327.35/4.88	364.50/7.57	197.69/2.71	233.99/3.90	260.62/5.41
$\mathcal{L}_0$ [ $10^{33}$ m $^{-2}$ ]	4.777	4.496	3.490	8.365	7.870	6.830
$A_x/A_y$	0.009/0.9	0.010/1.00	0.011/0.725	0.009/0.72	0.01/0.8	0.011/0.725
$D_x/D_y$	0.094/7.67	0.117/7.87	0.136/6.53	0.094/6.85	0.103/7.03	0.136/6.53
$\Upsilon_{avg}$	0.14	0.11	0.09	0.39	0.30	0.25
$\mathcal{L}_D$ [ $10^{33}$ m $^{-2}$ ]	6.51	5.84	5.21	12.57	11.36	10.24
$H_D \equiv \mathcal{L}_D/\mathcal{L}_0$	1.36	1.30	1.49	1.50	1.44	1.50
$n_\gamma$	1.08	1.18	1.24	1.39	1.53	1.62
$\delta_B$	4.3%	3.9%	3.7%	9.5%	9.2%	8.7%
Num. bunches per train	95	95	95	95	95	95
Repetition rate	120	120	120	120	120	120
$L_D$ [ $\text{cm}^{-2}\text{sec}^{-1}$ ]	7.42	6.66	5.94	14.33	12.95	11.67

$$\mathcal{L}_0 \equiv \frac{N^2}{4\pi\sigma_x\sigma_y} \quad . \quad (1)$$

Although the absolute luminosity is of course greatest for the nominal case, note that the luminosity enhancement  $H_D$  is less for the nominal case than for the cases with relaxed beta function, even though the disruption is larger. This is because the luminosity is reduced less by the hour-glass effect in the cases with relaxed beta function. The crossing of the  $H_D$  curves as one goes to larger  $y/\sigma_y$  is simply due to the fact that  $\sigma_y$  is  $\sqrt{2}$  larger for the relaxed beta function cases.

Figures 3 and 11 show the average beamstrahlung energy loss  $\delta_B$  as a function of  $y$ -offset. The initial increase of  $\delta_B$  with offset is due to the fact that particles in the core of one bunch are passing through the high-field region just outside the core of the other bunch.

Plots of luminosity per bunch  $\ell_D$ , luminosity enhancement  $H_D$ , and average beamstrahlung energy loss  $\delta_B$ , as a function of  $y$ -angle offsets, are shown in Figures 5 through 7 for NLC-B-500, and Figures 13 through 15 for NLC-B-1000, and similar remarks apply as in the case of position offsets. We show also  $n_\gamma$ , the number of beamstrahlung photons per incoming particle, in Figures 8 and 16; the behavior of  $n_\gamma$  is similar to that of  $\delta_B$ , for the same reason i.e., more particles are passing through the high field region as one begins to increase the offset.

The luminosity degradation for an offset of  $1\sigma_y$  is essentially the same for all cases, about 8% (see Table 2). The budgeted rms offset jitter for NLC is about

**TABLE 2.** Luminosity loss at vertical offsets of 1 and  $2\sigma_y$

	$1\sigma_y$ offset	$2\sigma_y$ offset
NLC-B-500	-7.6%	-20%
NLC-B-500, relax $\beta$	-8.3%	-24%
NLC-B-500, relax $\beta$ , lower $N$	-7.7%	-25%
NLC-B-1000	-8.3%	-23%
NLC-B-1000, relax $\beta$	-8.5%	-25%
NLC-B-1000, relax $\beta$ , lower $N$	-8.0%	-26%

**TABLE 3.** Luminosity loss at vertical angle offsets of 20 and 40  $\mu\text{rad}$

	20 $\mu\text{rad}$	40 $\mu\text{rad}$
NLC-B-500	-3.1%	-12.0%
NLC-B-500, relax $\beta$	-2.3%	-8.7%
NLC-B-500, relax $\beta$ , lower $N$	-2.2%	-8.4%
NLC-B-1000	-6.6%	-19.5%
NLC-B-1000, relax $\beta$	-3.8%	-13.5%
NLC-B-1000, relax $\beta$ , lower $N$	-4.1%	-12.6%

$0.7\sigma_y$ . Even at a  $2\sigma_y$  offset there is not very much difference among all the cases – the luminosity loss ranges from about 20 to 25%.

The luminosity loss for angle offsets of 20 and 40  $\mu\text{rad}$  is shown in Table 3. The budgeted rms angle jitter for NLC is about  $0.7\sigma'_y$ , which for NLC-B-500 is 30  $\mu\text{rad}$  and for NLC-B-1000 20  $\mu\text{rad}$ .

Thus the expected luminosity loss due to angle offsets is comparable to that due to position offsets, about 5% for each. Furthermore, the luminosity loss due to vertical angle offsets is even less with a relaxed  $\beta_y$  than with the nominal  $\beta_y$ . Thus relaxing the vertical beta function does not worsen the effect of offsets, even though the disruption is reduced, apparently because the reduced hour glass degradation is more important.

## REFERENCES

1. See <http://www-project.slac.stanford.edu/lc/nlc-tech.html> under Accelerator Physics parameters.
2. K.A.Thompson and T.O.Raubenheimer, “Luminosity for NLC Design Variations”, NLC note LCC-0014 (March, 1999).
3. D.Schulte, Ph.D. thesis, 1996.
4. Yokoya,K. and Chen,P., in M.Dienes,et.al. (ed.), Frontiers of Particle Beams: Intensity Limitations, (Springer-Verlag, 1992), p.415.

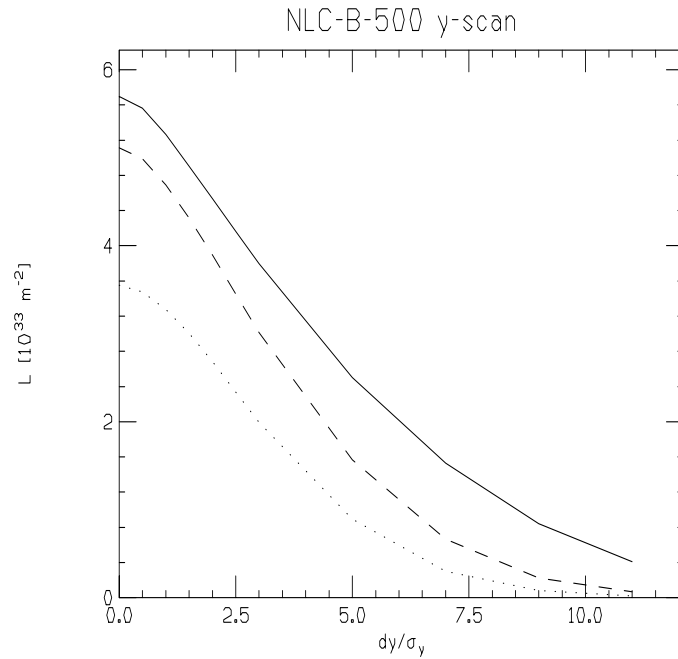


**FIGURE 1.** Luminosity (per bunch) for  $y$ -scan, shown versus  $dy/\sigma_y$ , for nominal NLC-B-500 (solid), NLC-B-500 with  $\beta_y = 0.24$  mm (dashed), NLC-B-500 with  $\beta_y = 0.24$  mm and  $N = 0.8 \times 10^{10}$  (dotted).

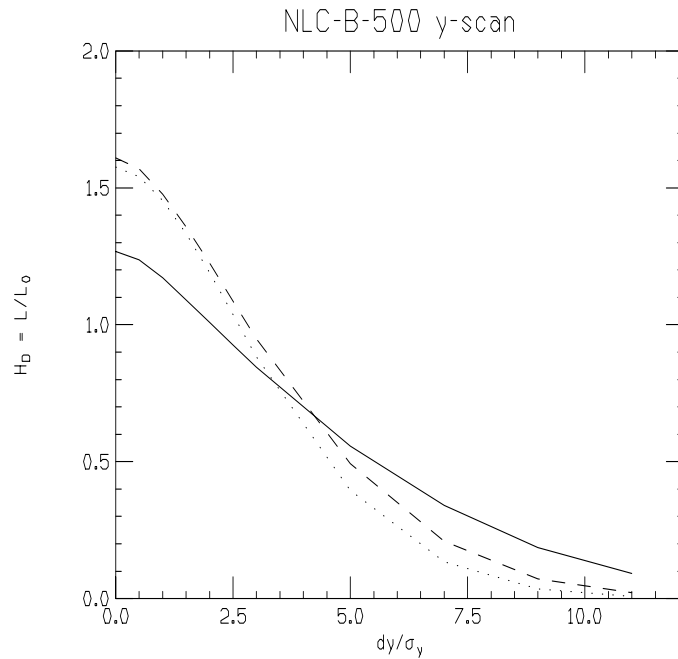


**FIGURE 2.** Enhancement factor  $H_D$  for  $y$ -scan for nominal NLC-B-500 (solid), NLC-B-500 with  $\beta_y = 0.24$  mm (dashed), NLC-B-500 with  $\beta_y = 0.24$  mm and  $N = 0.8 \times 10^{10}$  (dotted).

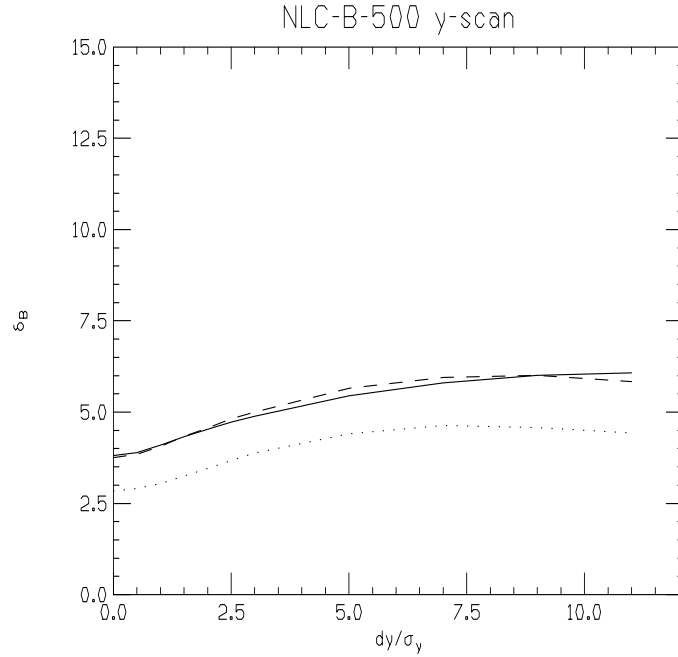


**FIGURE 3.** Average beamstrahlung energy loss for  $y$ -scan for nominal NLC-B-500 (solid), NLC-B-500 with  $\beta_y = 0.24$  mm (dashed), NLC-B-500 with  $\beta_y = 0.24$  mm and  $N = 0.8 \times 10^{10}$  (dotted).

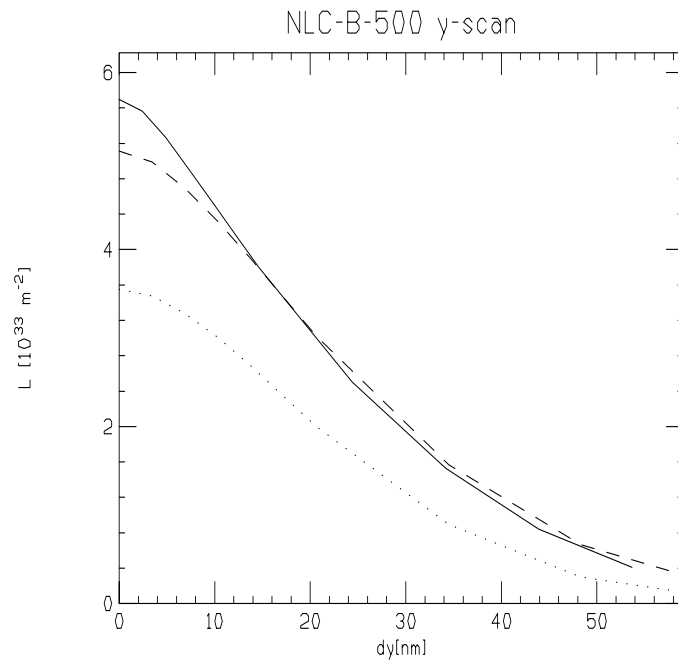


**FIGURE 4.** Luminosity (per bunch) for  $y$ -scan, shown versus  $dy$  in nanometers, for nominal NLC-B-500 (solid), NLC-B-500 with  $\beta_y = 0.24$  mm (dashed), NLC-B-500 with  $\beta_y = 0.24$  mm and  $N = 0.8 \times 10^{10}$  (dotted).

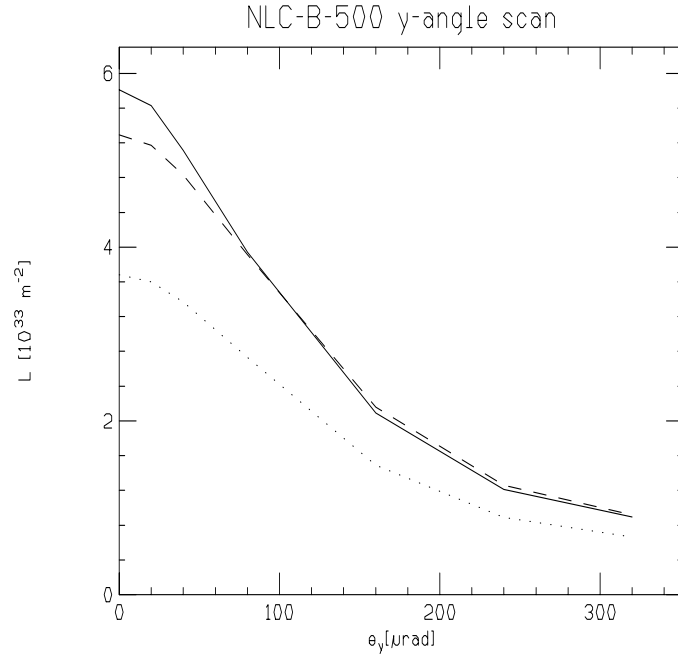


**FIGURE 5.** Luminosity (per bunch) for  $y$ -angle scan for nominal NLC-B-500 (solid), NLC-B-500 with  $\beta_y = 0.24$  mm (dashed), NLC-B-500 with  $\beta_y = 0.24$  mm and  $N = 0.8 \times 10^{10}$  (dotted).

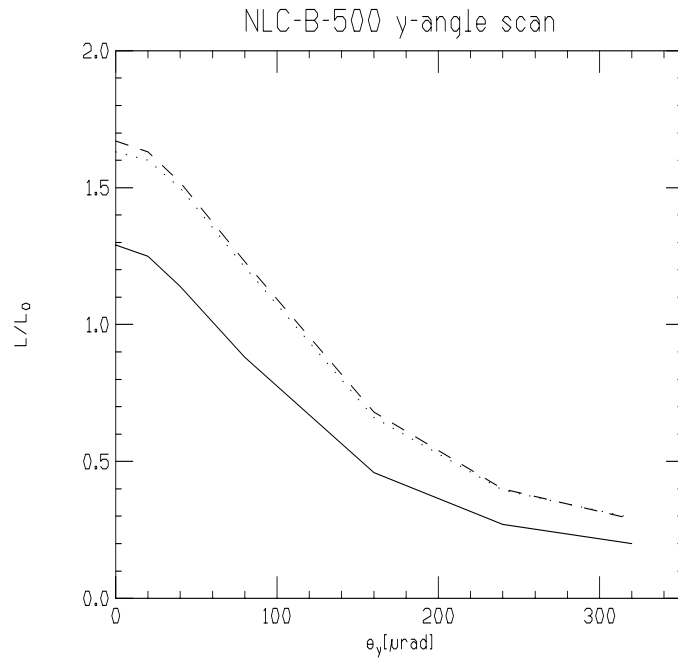


**FIGURE 6.** Enhancement factor  $H_D$  for  $y$ -angle scan for nominal NLC-B-500 (solid), NLC-B-500 with  $\beta_y = 0.24$  mm (dashed), NLC-B-500 with  $\beta_y = 0.24$  mm and  $N = 0.8 \times 10^{10}$  (dotted).

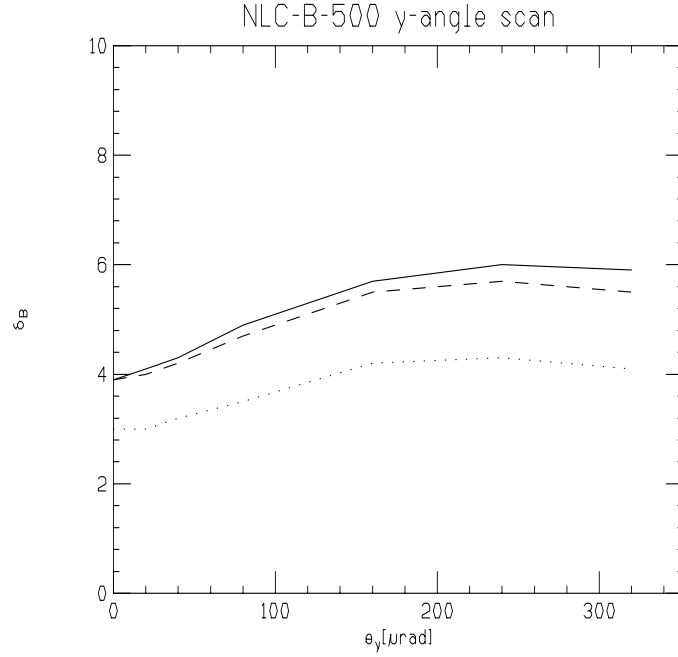


**FIGURE 7.** Average beamstrahlung energy loss for for  $y$ -angle scan for nominal NLC-B-500 (solid), NLC-B-500 with  $\beta_y = 0.24$  mm (dashed), NLC-B-500 with  $\beta_y = 0.24$  mm and  $N = 0.8 \times 10^{10}$  (dotted).

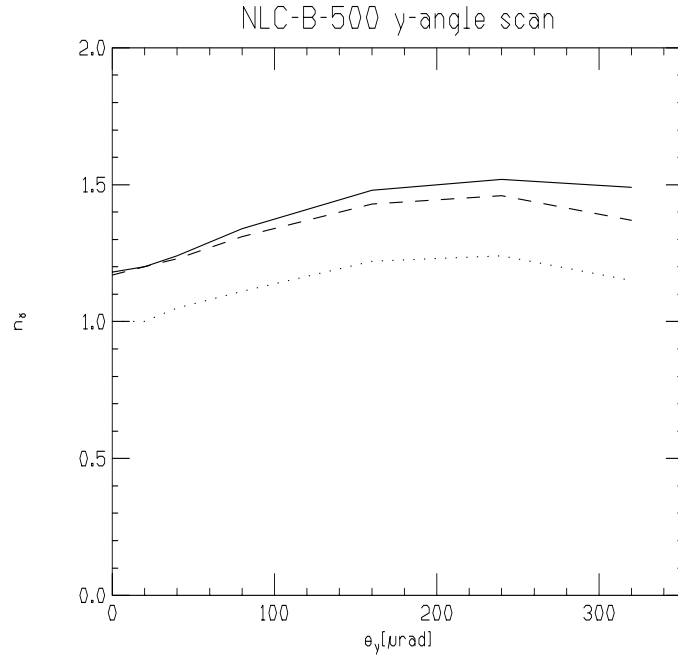


**FIGURE 8.** Average number of photons produced per incoming particle for  $y$ -angle scan for nominal NLC-B-500 (solid), NLC-B-500 with  $\beta_y = 0.24$  mm (dashed), NLC-B-500 with  $\beta_y = 0.24$  mm and  $N = 0.8 \times 10^{10}$  (dotted).



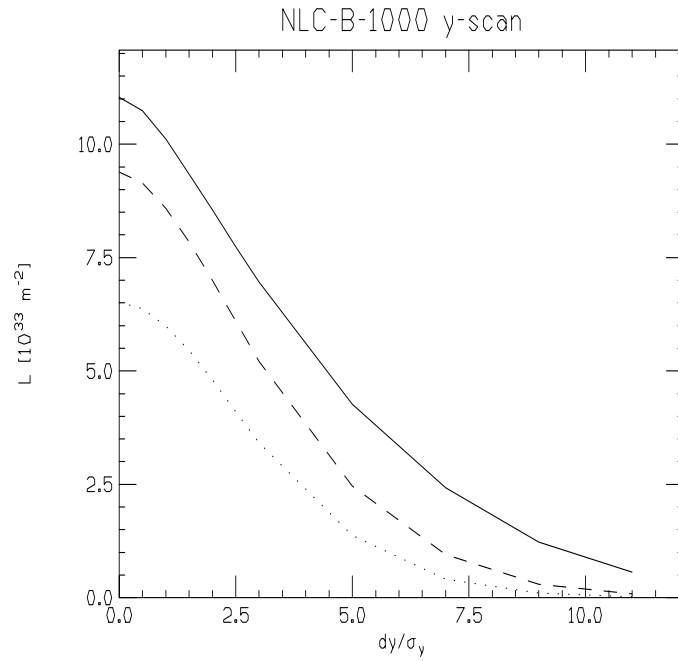


**FIGURE 9.** Luminosity (per bunch) for  $y$ -scan, shown versus  $dy/\sigma_y$ , for nominal NLC-B-1000 (solid), NLC-B-1000 with  $\beta_y = 0.30$  mm (dashed), NLC-B-1000 with  $\beta_y = 0.30$  mm and  $N = 0.8 \times 10^{10}$  (dotted).

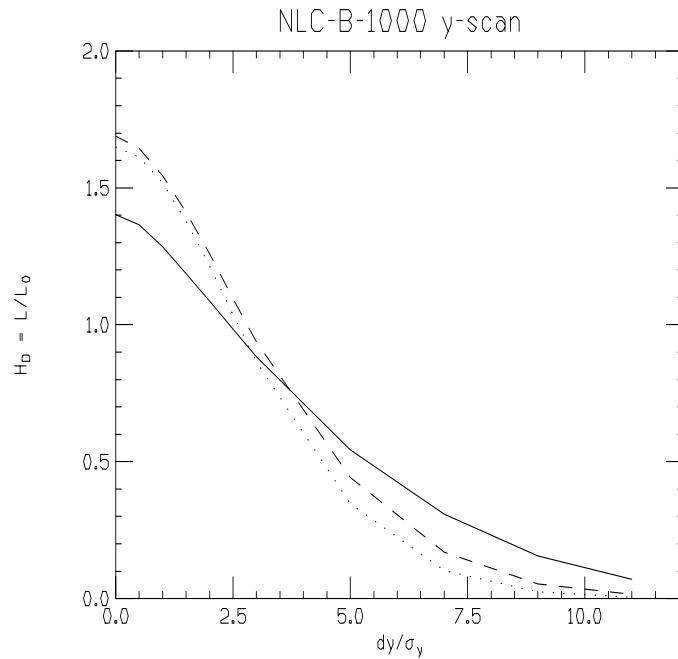


**FIGURE 10.** Enhancement factor  $H_D$  for  $y$ -scan, for nominal NLC-B-1000 (solid), NLC-B-1000 with  $\beta_y = 0.30$  mm (dashed), NLC-B-1000 with  $\beta_y = 0.30$  mm and  $N = 0.8 \times 10^{10}$  (dotted).

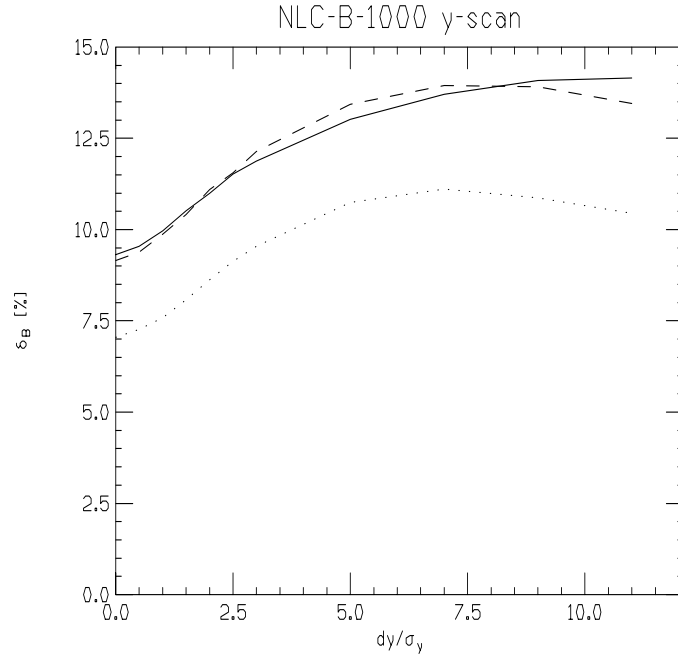


**FIGURE 11.** Average beamstrahlung energy loss for  $y$ -scan for nominal NLC-B-1000 (solid), NLC-B-1000 with  $\beta_y = 0.30$  mm (dashed), NLC-B-1000 with  $\beta_y = 0.30$  mm and  $N = 0.8 \times 10^{10}$  (dotted).

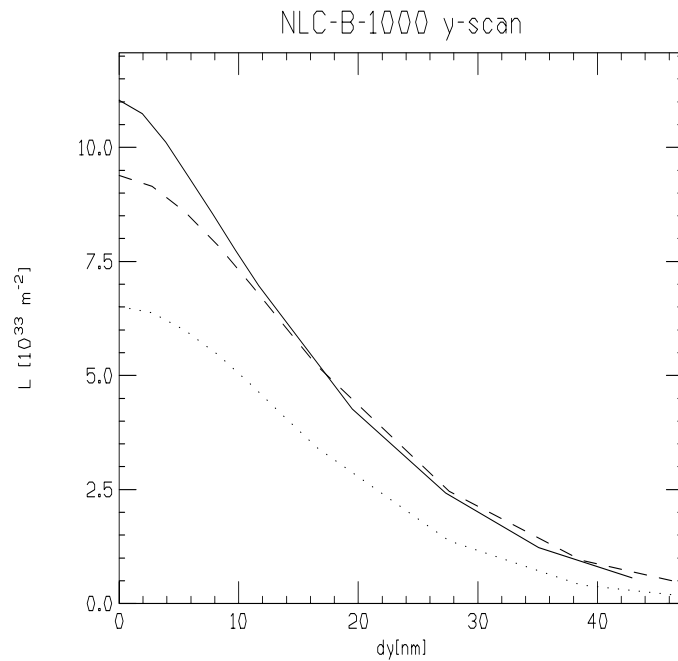


**FIGURE 12.** Luminosity (per bunch) for  $y$ -scan, shown versus  $dy$  in nanometers, for nominal NLC-B-1000 (solid), NLC-B-1000 with  $\beta_y = 0.30$  mm (dashed), NLC-B-1000 with  $\beta_y = 0.30$  mm and  $N = 0.8 \times 10^{10}$  (dotted).

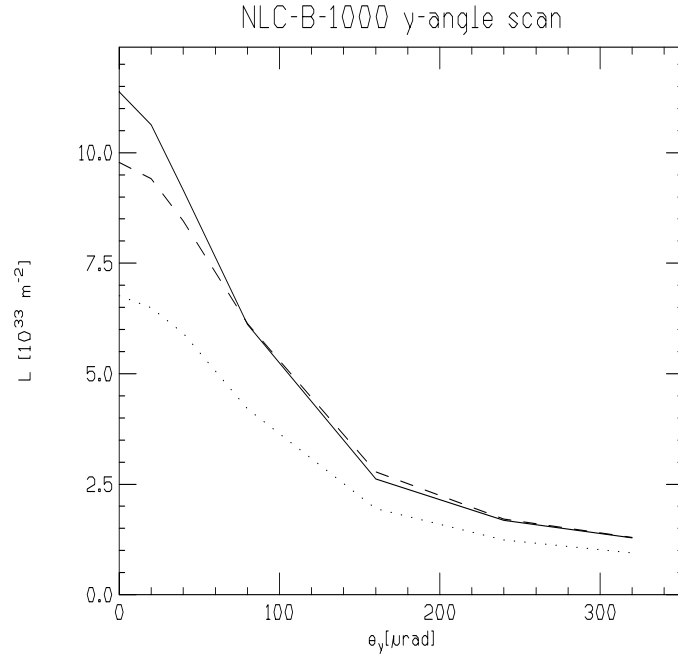


**FIGURE 13.** Luminosity (per bunch) for  $y$ -angle scan for nominal NLC-B-1000 (solid), NLC-B-1000 with  $\beta_y = 0.30$  mm (dashed), NLC-B-1000 with  $\beta_y = 0.30$  mm and  $N = 0.8 \times 10^{10}$  (dotted).

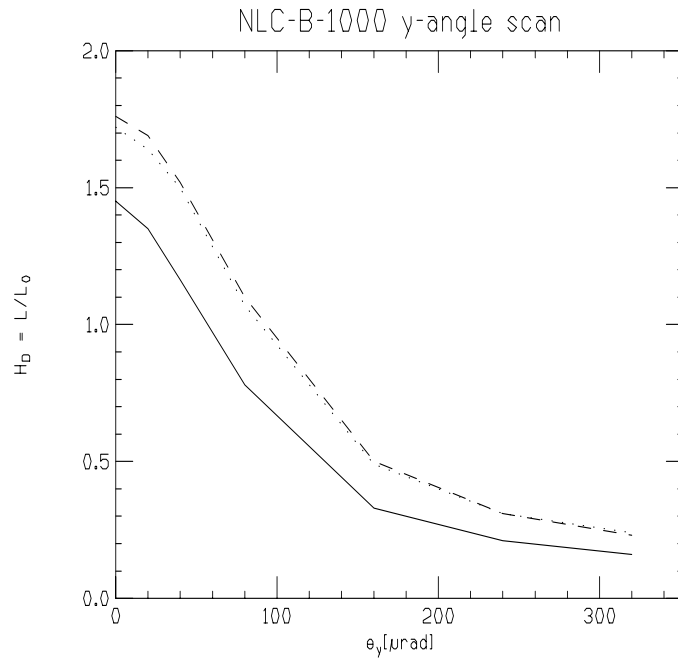


**FIGURE 14.** Enhancement factor  $H_D$  for  $y$ -angle scan for nominal NLC-B-1000 (solid), NLC-B-1000 with  $\beta_y = 0.30$  mm (dashed), NLC-B-1000 with  $\beta_y = 0.30$  mm and  $N = 0.8 \times 10^{10}$  (dotted).

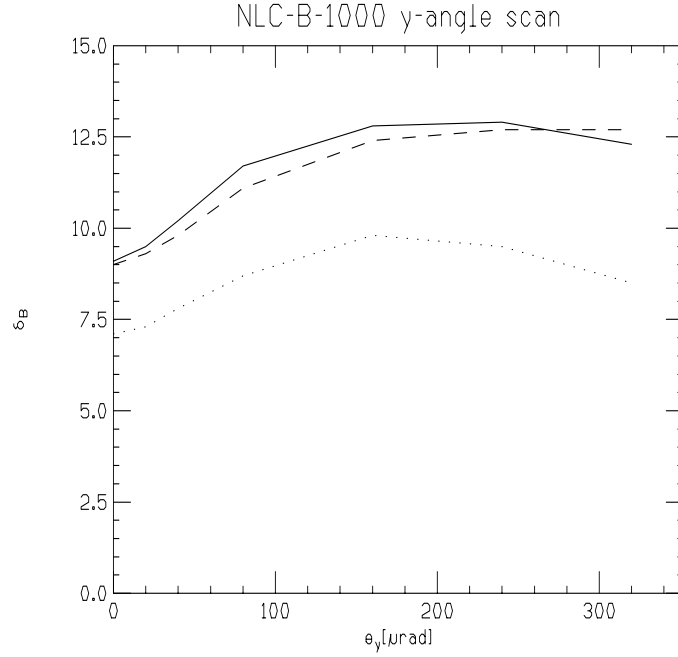


**FIGURE 15.** Average beamstrahlung energy loss for  $y$ -angle scan for nominal NLC-B-1000 (solid), NLC-B-1000 with  $\beta_y = 0.30$  mm (dashed), NLC-B-1000 with  $\beta_y = 0.30$  mm and  $N = 0.8 \times 10^{10}$  (dotted).

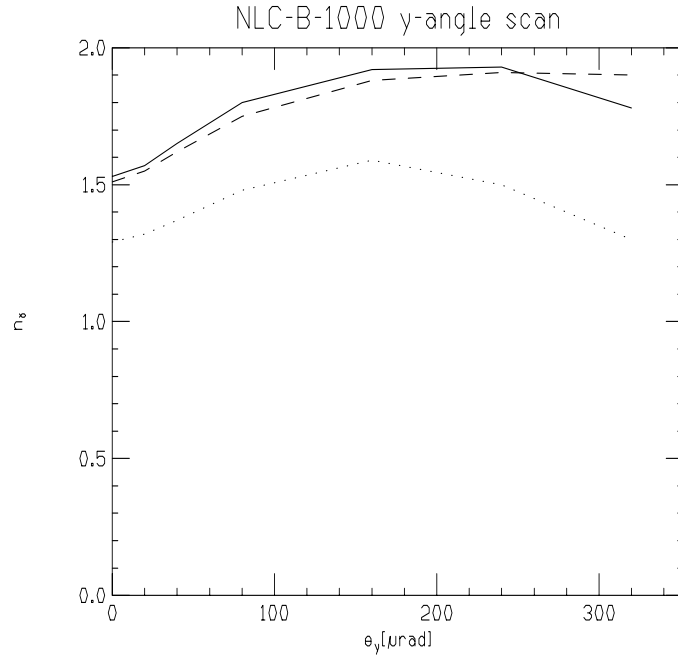


**FIGURE 16.** Average number of photons produced per incoming particle for  $y$ -angle scan for nominal NLC-B-1000 (solid), NLC-B-1000 with  $\beta_y = 0.30$  mm (dashed), NLC-B-1000 with  $\beta_y = 0.30$  mm and  $N = 0.8 \times 10^{10}$  (dotted).